

FORMATION OF INTERFEROGRAMS IN DIFFUSELY SCATTERED LIGHT DURING THE RECORDING OF THE GABOR HOLOGRAM USED FOR TESTING A TELESCOPIC OPTICAL SYSTEM

V.G. Gusev

*Tomsk State University
Received February 5, 1996*

An analysis of an interferometer has been performed based on recording of a hologram of an amplitude scatterer image focused according to the Gabor scheme with the Kepler telescope. It has been shown theoretically and experimentally that when performing the spatial filtration of a diffraction field, an interferogram characterizing spherical aberrations of a controllable object is formed in the hologram plane.

In Ref. 1 it was shown that the double-exposure recording of a hologram of a mat screen image focused with the Kepler telescope and produced by the off-axis reference wave at the stage of its reconstruction leads to the formation of shear interferograms in fringes of infinite width produced by diffusely scattered light fields. Each particular speckle in the hologram plane contains the information about aberrations of an optical system. When performing the spatial filtration of the diffraction field in the hologram plane, the interference pattern, which characterizes aberrations, is localized in the far diffraction zone. In its turn, the speckle field in this plane is modulated by a phase function determining the wave aberrations of the optical system in the channel of the reference wave formation and also in the channel where the radiation is formed used to illuminate the mat screen. The interference pattern characterizing these aberrations is localized in the hologram plane. To detect the interference pattern, it is necessary to perform spatial filtration of the diffraction light field in the plane of the Fourier transform of the mat screen image.

In the present paper, the conditions of formation of the interference pattern, which characterizes the spherical aberrations of an optical system of the Kepler telescope type, are analyzed. We consider the case of the single-exposure recording of a hologram of an image of an amplitude scatterer focused according to the Gabor scheme.

According to Fig. 1a the image of the amplitude scatterer 1 is formed on the photoplate 2 with the telescopic optical system that consists of two convergent lenses L_1 (the objective) and L_2 (the eyepiece). The recording of the Gabor hologram is performed when the scatterer is illuminated by coherent light. After development of the interferogram, it is illuminated by a plane wave from a coherent source used for its recording and in the Fourier plane 3 (Fig. 1b) the interference pattern is recorded when performing the spatial filtration of the diffraction field

on the optical axis in the hologram plane with the use of a circular aperture in the opaque screen P_3 .

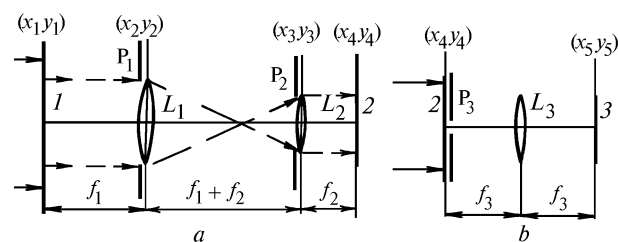


FIG. 1. Schematic diagram of recording (a) and reconstruction (b) of the Gabor hologram: amplitude scatterer 1, holographic photoplate 2, plane of hologram recording 3. Here, L_1 , L_2 , and L_3 are lenses, P_1 and P_2 are aperture stops, and P_3 is a spatial filter.

In general, the deformation of a recorded wavefront in case of displacement from the plane of the paraxial image depends on defocusing of the telescopic system, the angle of divergence (or convergence) of a spatially bounded coherent beam incident on the scatterer, the distance between the plane (x_1, y_1) and the principal plane (x_2, y_2) of the lens L_1 , and the distance between the principal plane (x_3, y_3) of the lens L_2 and the photoplate. However, consideration of all possible detunings in an analysis of real image formation leads to cumbersome expressions. So for brevity, we assume that the distance between the amplitude scatterer and the principal plane of the lens L_1 is $l_1 = f_1 \pm \Delta l_1$, where f_1 is the focal length of the lens L_1 and Δl_1 specifies the accuracy of scatterer positioning in the frontal focal plane of the lens L_1 . Hence, in the Fresnel approximation with allowance for diffraction limits using Eq. (1) and omitting the constant amplitude and phase factors, the complex amplitude in the photoplate plane can be represented in the following form:

$$\begin{aligned}
u(x_4, y_4) \sim & \exp\left[\frac{ik}{2f_2}(x_4^2 + y_4^2)\right] \times \\
& \times \left\{ \exp\left[-\frac{ik(f_1 + f_2)}{2f_2^2}(x_4^2 + y_4^2)\right] \times \right. \\
& \times \left\{ \exp\left[-\frac{ikl}{2f_2^2}(x_4^2 + y_4^2)\right] \left\{ [\delta(x_4, y_4) - F(x_4, y_4)] \otimes \right. \right. \\
& \otimes \Phi(x_4, y_4) \otimes \exp\left[-\frac{ikLl^2}{2l_1^2 f_2^2}(x_4^2 + y_4^2)\right] \left. \right\} \otimes P_1(x_4, y_4) \left. \right\} \otimes \\
& \otimes P_2(x_4, y_4) \left. \right\}, \quad (1)
\end{aligned}$$

where the symbol \otimes denotes the convolution operation, $\delta(x_4, y_4)$ is the Dirac delta function, k is the wave number, f_2 is the focal length of the lens L_2 ,

$$\frac{1}{l} = \frac{1}{l_1} - \frac{1}{f_1}, \quad \frac{1}{L} = \frac{1}{l_1} - \frac{1}{l_1^2},$$

$$\begin{aligned}
F(x_4, y_4) = & \iint_{-\infty}^{\infty} t(x_1, y_1) \times \\
& \times \exp\left[-\frac{ikl}{l_1 f_2}(x_1 x_4 + y_1 y_4)\right] dx_1 dy_1
\end{aligned}$$

is the Fourier transform of a real random function of coordinates that characterizes the absorption amplitude of the scatterer,

$$\begin{aligned}
\Phi(x_4, y_4) = & \iint_{-\infty}^{\infty} \exp[i\varphi_0(x_1, y_1)] \times \\
& \times \exp\left[-\frac{ikl}{l_1 f_2}(x_1 x_4 + y_1 y_4)\right] dx_1 dy_1
\end{aligned}$$

is the Fourier transform of a complex function, $\varphi_0(x_1, y_1)$ is a deterministic function characterizing the phase distortions introduced in the wavefront of radiation illuminating the amplitude scatterer by the aberrations of the optical system,

$$\begin{aligned}
P_1(x_4, y_4) = & \iint_{-\infty}^{\infty} P_1(x_2, y_2) \times \\
& \times \exp[i\varphi_1(x_2, y_2)] \exp\left[-\frac{ik}{f_2}(x_2 x_4 + y_2 y_4)\right] dx_2 dy_2
\end{aligned}$$

is the Fourier transform of the generalized pupil function² of the lens L_1 that takes into account its axial wave aberrations, and

$$\begin{aligned}
P_2(x_4, y_4) = & \iint_{-\infty}^{\infty} P_2(x_3, y_3) [\exp i\varphi_2(x_3, y_3)] \times \\
& \times \exp\left[-\frac{ik}{f_2}(x_3 x_4 + y_3 y_4)\right] dx_3 dy_3
\end{aligned}$$

is the Fourier transform of the generalized pupil function of the lens L_2 .

After representation of the convolution operation in the well-known integral form and taking the Fourier transform, Eq. (1) is converted to the form

$$\begin{aligned}
u(x_4, y_4) \sim & \exp\left[\frac{ik}{2f_2}(x_4^2 + y_4^2)\right] \times \\
& \times \left\{ \exp\left[-\frac{ik(f_1 + f_2)}{2f_2^2}(x_4^2 + y_4^2)\right] \times \right. \\
& \times \left\{ \exp\left[-\frac{ik(l_1^2 l + Ll^2)}{2l_1^2 f_2^2}(x_4^2 + y_4^2)\right] \times \right. \\
& \times \left\{ [1 - t(-\mu_1 x_4, -\mu_1 y_4)] \exp[i\varphi_0(-\mu_1 x_4, -\mu_1 y_4)] \otimes \right. \\
& \otimes \exp\left[\frac{ikLl^2}{2l_1^2 f_2^2}(x_4^2 + y_4^2)\right] \left. \right\} P_1(x_4, y_4) \left. \right\} \otimes P_2(x_4, y_4) \left. \right\}, \quad (2)
\end{aligned}$$

where $\mu_1 = ll_1/(l - l_1)f_2$ is the scale factor of image transformation.

For a diffusely scattered component of the field the width of the function $P_1(x_1, y_1)$ is of the order of $\lambda f_2/d_1$ (Ref. 3), where λ is the wavelength of the coherent light source used for recording and reconstruction of the hologram, d_1 is the pupil diameter of the lens L_1 . If in the existence domain of function $P_1(x_4, y_4)$ the phase change of a spherical wave with a curvature radius $l_1^2 f_2^2/(ll_1^2 + Ll^2)$ does not exceed π , this condition holds in the photoplate plane in a region with diameter $D_1 \leq d_1 l_1^2 f_2^2/(ll_1^2 + Ll^2)$. In this case, $\exp\left[-\frac{ikl(l_1^2 + Ll)}{2l_1^2 f_2^2}(x_4^2 + y_4^2)\right]$ can be taken outside the convolution integral with function $P_1(x_4, y_4)$. As a result, we obtain

$$\begin{aligned}
u(x_4, y_4) \sim & \exp\left[\frac{ik}{2f_2}(x_4^2 + y_4^2)\right] \times \\
& \times \left\{ \left[-\frac{ik(l_1^2 f_1 + l_1^2 f_2 + ll_1^2 + Ll^2)}{2l_1^2 f_2^2}(x_4^2 + y_4^2) \right] \times \right. \\
& \times \left\{ [1 - t(-\mu_1 x_4, -\mu_1 y_4)] \exp[i\varphi_0(-\mu_1 x_4, -\mu_1 y_4)] \otimes \right. \\
& \otimes \exp\left[\frac{ikLl^2}{2l_1^2 f_2^2}(x_4^2 + y_4^2)\right] \otimes P_1(x_4, y_4) \left. \right\} \otimes P_2(x_4, y_4) \left. \right\}. \quad (3)
\end{aligned}$$

Because the width of function $P_2(x_4, y_4)$ is of the order of $\lambda f_2/d_2$, where d_2 is the pupil diameter of the lens L_2 , in the existence domain of function $P_2(x_4, y_4)$ the phase change of the spherical wave with curvature radius $l_1^2 f_2^2/(l_1^2 f_1 + l_1^2 f_2 + ll_1^2 + Ll^2)$ does not exceed π for a region of plane (x_4, y_4) with diameter

$$D_2 \leq \frac{d_2 l_1^2 f_2}{l_1^2 f_1 + l_1^2 f_2 + ll_1^2 + Ll^2}.$$

In Eq. (3) we may take the factor $\exp\left[-\frac{ik(l_1^2 f_1 + l_1^2 f_2 + ll_1^2 + Ll^2)}{2l_1^2 f_2^2}(x_4^2 + y_4^2)\right]$ with function $P_2(x_4, y_4)$ outside the convolution integral. Assuming that $d_1 = d_2 f_1/f_2$, the distribution of the field complex amplitude in the region with diameter D_2 of the photoplate plane can be written as

$$u(x_4, y_4) \sim \exp \left[-\frac{ik(l_1^2 f_1 + ll_1^2 + Ll^2)}{2l_1^2 f_2^2} (x_4^2 + y_4^2) \right] \times \\ \times \left\{ [1 - t(-\mu_1 x_4, -\mu_1 y_4)] \exp[i\varphi_0(-\mu_1 x_4, -\mu_1 y_4)] \otimes \right. \\ \left. \otimes \exp \left[\frac{ikLl^2}{2l_1^2 f_2^2} (x_4^2 + y_4^2) \right] \otimes P_1(x_4, y_4) \otimes P_2(x_4, y_4) \right\}. \quad (4)$$

Let us also assume that to produce a negative, an emulsion layer that was exposed to light with the intensity $I(x_4, y_4) = u(x_4, y_4) u^*(x_4, y_4)$ was then developed in the region of the characteristic curve with the constant light sensitivity. Then for $t(x_1, y_1) \ll 1$ (Ref. 4), the transmission amplitude of the hologram $\tau(x_4, y_4)$ (Fig. 1b) is determined by the following expression:

$$\tau(x_4, y_4) \sim \left\{ \exp[i\varphi_0(-\mu_1 x_4, -\mu_1 y_4)] \otimes \right. \\ \left. \otimes \exp \left[\frac{ikLl^2}{2l_1^2 f_2^2} (x_4^2 + y_4^2) \right] \otimes P_1(x_4, y_4) \otimes P_2(x_4, y_4) \right\} \times \\ \times \left\{ t(-\mu_1 x_4, -\mu_1 y_4) \exp[-i\varphi_0(-\mu_1 x_4, -\mu_1 y_4)] \otimes \right. \\ \left. \otimes \exp \left[-\frac{ikLl^2}{2l_1^2 f_2^2} (x_4^2 + y_4^2) \right] \otimes P_1^*(x_4, y_4) \otimes P_2^*(x_4, y_4) \right\} + \\ + \left\{ \exp[-i\varphi_0(-\mu_1 x_4, -\mu_1 y_4)] \otimes \exp \left[-\frac{ikLl^2}{2l_1^2 f_2^2} (x_4^2 + y_4^2) \right] \otimes \right. \\ \left. \otimes P_1^*(x_4, y_4) \otimes P_2^*(x_4, y_4) \right\} \times \\ \times \left\{ t(-\mu_1 x_4, -\mu_1 y_4) \exp[i\varphi_0(-\mu_1 x_4, -\mu_1 y_4)] \otimes \right. \\ \left. \otimes \exp \left[\frac{ikLl^2}{2l_1^2 f_2^2} (x_4^2 + y_4^2) \right] \otimes P_1(x_4, y_4) \otimes P_2(x_4, y_4) \right\}. \quad (5)$$

The regular component of light transmission is omitted here because in the recording plane it influences only the illuminance of a small spot.

According to Ref. 5 the distribution of the complex amplitude of the diffusely scattered component of light field in the rear focal plane (x_5, y_5) of the lens L_3 with the focal length f_3 (Fig. 1b) can be written as

$$u(x_5, y_5) \sim \iint_{-\infty}^{\infty} \tau(x_4, y_4) \exp \left[-\frac{ik}{f_3} (x_4 x_5 + y_4 y_5) \right] \times \\ \times dx_4 dy_4 \otimes P_3(x_5, y_5), \quad (6)$$

where

$$P_3(x_5, y_5) = \iint_{-\infty}^{\infty} P_3(x_4, y_4) \times \\ \times \exp \left[-\frac{ik}{f_3} (x_4 x_5 + y_4 y_5) \right] dx_4 dy_4$$

is the Fourier transform of the transmission function of the opaque screen P_3 with a circular aperture.⁶

As a result of substitution of Eq. (5) into Eq. (6), we obtain

$$u(x_5, y_5) \sim \left\{ \left\{ \Phi_1(x_5, y_5) \exp \left[-\frac{ikl_1^2 f_2^2}{2Ll^2 f_3^2} (x_5^2 + y_5^2) \right] \times \right. \right. \\ \times P_1(\mu_2 x_5, \mu_2 y_5) P_2(\mu_2 x_5, \mu_2 y_5) \times \\ \left. \left. \times \exp i [\varphi_1(-\mu_2 x_5, -\mu_2 y_5) + \varphi_2(-\mu_2 x_5, -\mu_2 y_5)] \right\} \otimes \right. \\ \left. \otimes \left\{ [F_1(x_5, y_5) \otimes \Phi_2(x_5, y_5)] \exp \left[\frac{ikl_1^2 f_2^2}{2Ll^2 f_3^2} (x_5^2 + y_5^2) \right] \times \right. \right. \\ \times P_1(\mu_2 x_5, \mu_2 y_5) P_2(\mu_2 x_5, \mu_2 y_5) \times \\ \left. \left. \times \exp -i [\varphi_1(\mu_2 x_5, \mu_2 y_5) + \varphi_2(\mu_2 x_5, \mu_2 y_5)] \right\} + \right. \\ \left. + \left\{ \Phi_2(x_5, y_5) \exp \left[\frac{ikl_1^2 f_2^2}{2Ll^2 f_3^2} (x_5^2 + y_5^2) \right] \times \right. \right. \\ \times P_1(\mu_2 x_5, \mu_2 y_5) P_2(\mu_2 x_5, \mu_2 y_5) \times \\ \left. \left. \times \exp -i [\varphi_1(\mu_2 x_5, \mu_2 y_5) + \varphi_2(\mu_2 x_5, \mu_2 y_5)] \right\} \otimes \right. \\ \left. \otimes \left\{ [F_1(x_5, y_5) \otimes \Phi_1(x_5, y_5)] \exp \left[-\frac{ikl_1^2 f_2^2}{2Ll^2 f_3^2} (x_5^2 + y_5^2) \right] \times \right. \right. \\ \times P_1(\mu_2 x_5, \mu_2 y_5) P_2(\mu_2 x_5, \mu_2 y_5) \times \\ \left. \left. \times \exp i [\varphi_1(-\mu_2 x_5, -\mu_2 y_5) + \varphi_2(-\mu_2 x_5, -\mu_2 y_5)] \right\} \right\} \otimes \\ \otimes P_3(x_5, y_5), \quad (7)$$

where $\mu_2 = f_2/f_3$ is the scale factor of image transformation,

$$F_1(x_5, y_5) = \iint_{-\infty}^{\infty} t(-\mu_1 x_4, -\mu_1 y_4) \times \\ \times \exp \left[-\frac{ik}{f_3} (x_4 x_5 + y_4 y_5) \right] dx_4 dy_4, \\ \Phi_1(x_5, y_5) = \iint_{-\infty}^{\infty} \exp[i\varphi_0(-\mu_1 x_4, -\mu_1 y_4)] \times \\ \times \exp \left[-\frac{ik}{f_3} (x_4 x_5 + y_4 y_5) \right] dx_4 dy_4,$$

$$\Phi_2(x_5, y_5) = \iint_{-\infty}^{\infty} \exp[-i \varphi_0(-\mu_1 x_4, -\mu_1 y_4)] \times \exp\left[-\frac{ik}{f_3}(x_4 x_5 + y_4 y_5)\right] dx_4 dy_4$$

are the Fourier transforms of corresponding functions.

For a small enough existence domain of functions $\Phi_1(x_5, y_5)$ and $\Phi_2(x_5, y_5)$, we may set $\Phi_1(x_5, y_5) = \Phi_2(x_5, y_5) = \delta(x_5, y_5)$. This condition holds if during the hologram recording the period of variation of the function $\exp i \varphi_0(-\mu_1 x_4, -\mu_1 y_4)$ is greater than the size of any subjective speckle in the photoplate plane. Then within the limits of the image of the pupil of lens L_2 the distribution of the diffraction field is determined by the expression:

$$u(x_5, y_5) \sim \left\{ \exp\left[\frac{ik l_1^2 f_2^2}{2 L l^2 f_3^2}(x_5^2 + y_5^2)\right] \times \exp - i [\varphi_1(\mu_2 x_5, \mu_2 y_5) + \varphi_2(\mu_2 x_5, \mu_2 y_5)] + \exp\left[-\frac{ik l_1^2 f_2^2}{2 L l^2 f_3^2}(x_5^2 + y_5^2)\right] \exp i[\varphi_1(-\mu_2 x_5, -\mu_2 y_5) + \varphi_2(-\mu_2 x_5, -\mu_2 y_5)] \right\} F_1(x_5, y_5) \otimes P_3(x_5, y_5), \quad (8)$$

which describes the complex amplitude of the light field. The illuminance produced by this field in the plane of the Fourier transform 3 (Fig. 1b) has the subjective speckle-pattern with speckle size determined by the width of function $P_3(x_5, y_5)$. Similarly to Ref. 1 assuming that the speckle size is much smaller than the period of variation of function that modulates the speckle pattern (in Eq. (8), the period of variation is characterized by the term in curly brackets), the illuminance distribution in the rear focal plane of lens L_3 can be represented as

$$I(x_5, y_5) \sim \left\{ 1 + \cos \left\{ -\left[\frac{k l_1^2 f_2^2}{L l^2 f_3^2}(x_5^2 + y_5^2)\right] + 2 \varphi_1(\mu_2 x_5, \mu_2 y_5) + 2 \varphi_2(\mu_2 x_5, \mu_2 y_5) \right\} \right\} \times |F_1(x_5, y_5) \otimes P_3(x_5, y_5)|^2. \quad (9)$$

It follows from Eq. (9) that the subjective speckle-pattern in the Fourier plane is modulated by interference fringes. When $\varphi_1(x_2, y_2) = \varphi_2(x_3, y_3) = 0$, the interference pattern has the form of the Young fringes⁷ with quadratic dependence of the interference fringe period on the radius. If $d_2 \leq (l/l_1) \sqrt{2 \lambda L}$, the illuminance distribution in the recording plane is governed by the expression

$$I(x_5, y_5) \sim \{1 + \cos [2 \varphi_1(\mu_2 x_5, \mu_2 y_5) + 2 \varphi_2(\mu_2 x_5, \mu_2 y_5)]\} |F_1(x_5, y_5) \otimes P_3(x_5, y_5)|^2, \quad (10)$$

where $\varphi_1(x_2, y_2) = \frac{k}{4} B_1(x_2^2 + y_2^2)^2$, $\varphi_2(x_3, y_3) = \frac{k}{4} B_2(x_3^2 + y_3^2)^2$ (Ref. 6). Here, B_1 and B_2 are the coefficients of the third-order spherical aberrations due to lenses L_1 and L_2 written in designations accepted in Ref. 7. In this case, the interference pattern in fringes of identical widths has the form of concentric fringes. The period of fringes is proportional to the radius in the fourth power.

In our experiments, the hologram was recorded on photoplates of the Mikrat VRL type by the He-Ne laser radiation with a wavelength of 0.63 μm . The real image of the amplitude scatterer was formed with a telescopic system that included two identical convergent lenses with focal lengths $f_1 = f_2 = f = 180$ mm, pupil diameters of 25 mm, and the coefficients of spherical aberration $b_1 = b_2 = 7\lambda$ (Ref. 8) expressed in wavelengths. The diameter of the illuminated area of the amplitude scatterer was 35 mm.

In Fig. 2, the interference pattern is shown that was recorded in the focal plane of a camera objective with a focal length of 50 mm when performing the spatial filtration of the diffraction field in the hologram plane on the optical axis in the process of reconstruction of the hologram with the use of a small-aperture (about 2 mm) laser beam. Recording of the hologram was performed in the plane of the best position that corresponds to the paraxial image of the amplitude scatterer. Based on the above estimation of the accuracy for the scatterer position in the frontal plane of lens L_1 (Fig. 1a), the recording of a series of holograms was performed with the step $\Delta l_1 = 0.1$ mm. In contrast to Fig. 2a where the interference pattern was due to spherical aberration of the optical system, in Fig. 2b the interference pattern was recorded during the hologram reconstruction on the optical axis by a small-aperture laser beam for a displacement from the best position plane of 2 mm. This pattern primarily characterizes defocusing.

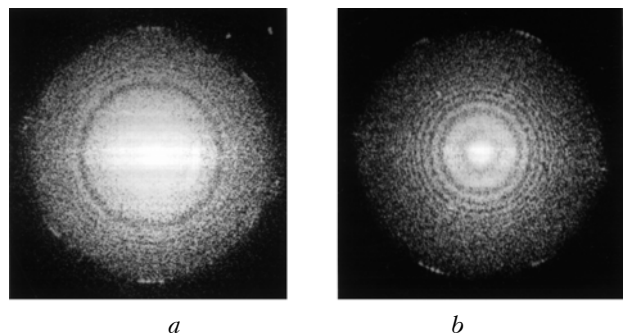


FIG. 2. Interference patterns that characterize spherical aberration (a) and primarily defocusing (b) of a controllable object.

The interference patterns of the interferometer under consideration are similar to that of the classical Twyman-Green interferometer that is employed for testing of a wave front shape and recording of spherical aberrations of telescopic system.⁹ But the physical nature of interference patterns is different. Thus, the Twyman-Green interferometer is used to compare the reference and controllable wave fronts. The latter is formed in the active channel of the interferometer due to double passage of the reference wave through a controllable object. The resulting interference fringes with identical widths characterize the quality of the telescopic optical system.

According to Eq. (4), for the holographic interferometer each speckle in the hologram plane contains all information on phase aberrations introduced in a light wave by the Kepler telescope. For a small region of the amplitude scatterer image on the optical axis, the field distribution within each speckle is a result of the plane wave diffraction by the pupils of the objective and eyepiece of the telescope. It is assumed that the plane wave propagates along the optical axis. So according to Eq. (7), the waves in the plus- and minus- first orders of diffraction have the same propagation directions but their wave fronts are conjugate and turned through an angle of 180° relative to each other about the optical axis. Due to this fact, we observe the interference of two axially symmetric wave fronts. The sensitivity of such measurements is no worse than that of the Twyman-Green interferometer, but the phase difference of two interfering wave fronts is always zero on the optical axis. Moreover, it is not necessary to use a reference wave with a wave front of high optical quality.

When the hologram is reconstructed at a point displaced from the optical axis, for example, at a point with coordinates $(x_{40}, 0)$, for all speckles in the vicinity of this point the amplitude-phase distribution of the field is a result of diffraction of a wave scattered with spatial frequency $x_{40}/\lambda f$ in the object plane (for the case of unit magnification).

Because the optical system of the Kepler telescope restricts the angular spectrum of scattered waves, wave fronts in the plus- and minus- first diffraction orders are turned additionally through the angle $\alpha = 2 x_{40}/\lambda f$ relative to each other. For these diffraction orders, additional phase difference arises on the x axis between axially symmetric wave fronts (here we ignore the off-axis aberrations, because the sensitivity of the interferometer to such aberrations is low). The phase difference is equal for points symmetric about the point at which the hologram is reconstructed by a small-aperture laser beam.

Such a situation is illustrated by Fig. 3, where the interference pattern is shown that has been recorded in the focal plane of the camera during the hologram reconstruction at the point displaced from the optical

axis by 6 mm. Therefore, the observation of the interference patterns described by Eqs. (9) and (10) is possible only in the hologram plane when performing the spatial filtration of the diffraction field on the optical axis. Moreover, the higher is the coefficient of spherical aberration that characterizes the quality of optical system, the smaller should be the diameter of the spatial filter aperture P_3 (see Fig. 1b). In its turn, this leads to the increased speckle size in the observation plane for a fixed focal length of the lens L_3 . When the speckle size becomes close to the width of the interference fringe, the interference pattern is no longer seen.¹⁰ Because of this fact, in Fig. 2 the interference fringes corresponding to higher orders of interference are absent on the periphery of the image of the output pupil. Estimation for the spherical aberration made for the low interference orders in the optical system under control have shown that it is within 14λ .

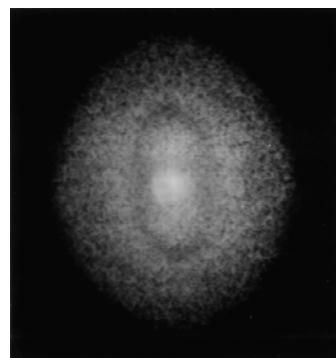


FIG. 3. Interference pattern localized in the far diffraction zone when performing the off-axis spatial filtration in the hologram plane.

Therefore, our investigations allow us to conclude that during the single-exposure recording of the hologram of the amplitude scatterer image focused by the Kepler telescope, in the best position plane corresponding to the recording of a paraxial image, at the stage of its restoration the interference pattern in fringes with identical widths is formed which characterizes the spherical aberrations of the object under control. For its observations, the spatial filtration of the field in the hologram plane is necessary on the optical axis. The filtration is required to ensure the coincidence of conjugate wave fronts turned through an angle of 180° relative to each other about the optical axis in the plus- and minus- first orders of diffraction. The interference pattern that modulates the speckle-structure in the Fourier plane is produced by superposition of these wave fronts. To observe the higher orders of interference, the camera objectives with shorter focal lengths are required.

REFERENCES

1. V.G. Gusev, *Atm. Opt.* **4**, No. 5, 360–366 (1991).
2. D. Goodman, *Introduction to the Fourier Optics* [Russian translation] (Mir, Moscow, 1970), 359 pp.
3. M. Franson, *Optics of Speckles* [Russian translation] (Mir, Moscow, 1980), 158 pp.
4. D. Gabor, *Nature* **161**, 777–778 (1948).
5. V.G. Gusev, *Opt. Spektrosk.* **69**, No. 5, 1125–1128 (1990).
6. M. Born and E. Wolf, *Principles of Optics* (Pergamon Press, New York, 1966).
7. M. Franson, *Holography* [Russian translation] (Mir, Moscow, 1972), 195 pp.
8. V.G. Gusev, *Izv. Vyssh. Uchebn. Zaved. SSSR, Ser. Fizika*, No. 9 (1996), (in press).
9. D. Malakara, ed., *Optical Testing* (Mashinostroenie, Moscow, 1985), 400 pp.
10. R. Jones and K. Wyks, *Holographic and Speckle Interferometry* [Russian translation] (Mir, Moscow, 1986), 320 pp.